

# Measurement of Double Differential Cross Section for Proton Emission Reactions of Silicon and Fluorine by Incident DT Neutrons

Yasuaki Terada, Hiroyuki Takagi, Isao Murata, Akito Takahashi  
Department of Nuclear Engineering, Osaka University  
Yamadaoka 2-1, Suita, Osaka, 565-0871, Japan  
e-mail: terada@newjapan.nucl.eng.osaka-u.ac.jp

In OKTAVIAN, the Intense 14MeV Neutron Source Facility of Osaka University, the double differential cross sections (DDXs) of (n,xp) reaction for  $^{nat}\text{Si}$ ,  $^{19}\text{F}$  induced by incident DT neutrons have been measured by using by two-dimensional analysis of the E-TOF spectrum, combined with the pulse-shape discrimination technique. From the result of comparison with JENDL fusion file, JENDL fusion file fairly reproduced the shape of the spectra, however, a slight underestimation was observed.

## 1. Introduction

In fusion power reactor development, it is indispensable to understand behavior of charged particles, because the DDX of charged particles emission reactions (DDXc) induced by 14 MeV incident neutrons is of primary importance for evaluation of nuclear heating and material damages in the elements and components of DT fusion devices. However, until now only a few data have been measured worldwide because of experimental difficulties such as high background and low net-count rate due to small cross section and thin sample.

In the previous experiments, we could use relatively thin samples because they were mostly medium-heavy metals. However, in light elements, a thin sample cannot be prepared easily and the thickness of their compounds available becomes more than a few hundred micrometers. In the last few years, the new unfolding method (spectrum type Bayes estimation method [1]) was therefore introduced to realize measurements with a thick sample [2]. The

purpose of this study is to measure the DDXs of proton emission reaction from  $^{nat}\text{Si}$ (320  $\mu\text{m}$ ) and  $^{19}\text{F}$ (500  $\mu\text{m}$ ) by using the spectrum type Bayes estimation method and

**Table.1 Description of the measured samples**

Sample nucleus	Measured particle	Sample material	Measured angle (deg)	$\phi$ (mm)	Thickness ( $\mu\text{m}$ )	Abundance (%)
$^{19}\text{F}$	Proton	Teflon	45, 60, 70, 90, 110	60.0	500	$^{19}\text{F}$ 100.0
$^{nat}\text{Si}$	Proton	Si wafer	45, 60, 70, 90, 110	28.0	320	$^{28}\text{Si}$ 92.23 $^{29}\text{Si}$ 4.67 $^{30}\text{Si}$ 3.10

E-TOF method combined with the pulse-shape discrimination technique [3]. Silicon is a very important semiconductor material and can be used as a plasma facing material (SiC), blanket material ( $\text{Li}_2\text{SiO}_3$ ), and so on. Fluorine is well known as is contained in FLIBE ( $\text{Li}_2\text{BeF}_4$ ), which is one of the famous liquid blanket materials. The details of the samples are shown in Table 1.

## 2. Experimental procedure

The charged-particle spectrometer, the schematic view of which is shown in Fig.1, was arranged in a cylindrical vacuum chamber of 1 m in diameter and 1 m in length. The chamber was kept at a pressure of  $\sim 1.3$  Pa. The background counts in charged-particle detection were reduced by the pulse-shape discrimination technique and shielding set made of iron, lead and polyethylene. The detector was placed inside the lead shield. The particle-emission angle can be changed by adjusting the sample position as shown in Fig.2. The flight path of emitted particle varies from 42 cm to 59 cm according to the emission angle. The measurements of the DDXc were carried out at five angles of 45, 60, 70, 90 and 110 deg.

As neutron source, pulsed D-T neutrons at OKTAVIAN of Osaka University were used. The OKTAVIAN generates  $5 \times 10^8$  neutrons/s by bombarding a 370 GBq TiT target using pulsed deuteron beams with  $\sim 3$  ns pulse width and 2 MHz repetition frequency. The TiT target was positioned in a stainless steel through-tube and out of the vacuum chamber.

A CsI(Tl) scintillator (1.5 mm in thickness and 50 mm in diameter) was used as charged-particle detector because of its good performance in pulse-shape discrimination.

Figure 3 shows the electronic circuit for the present measurement. The two-dimensional data acquisition has been done by using the pulse height of the dynode signal corresponding to energy and the TOF signal. The latter was created by the time-to-pulse-height converter using the fast signals of the anode as the start signal and the stop signal (with delay) from the trigger pulse of the deuteron beam. The logic signal created by the pulse-shape discrimination circuit has been fed as the gate signal to extract the charged particle of interest.

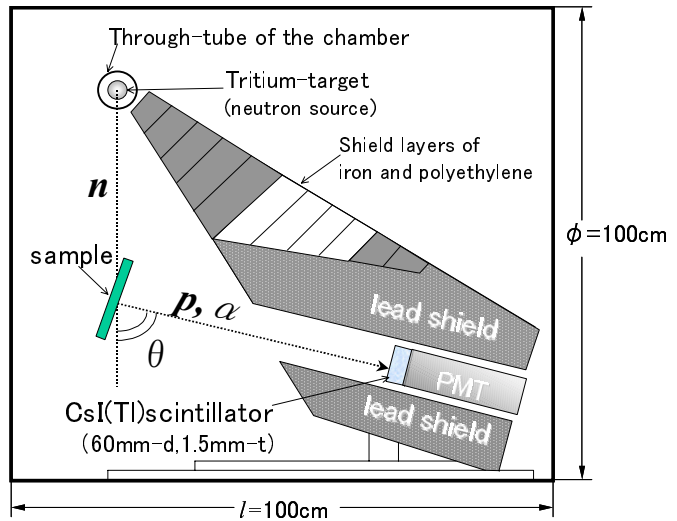


**Fig.1 Schematic arrangement of the charged particle spectrometer**

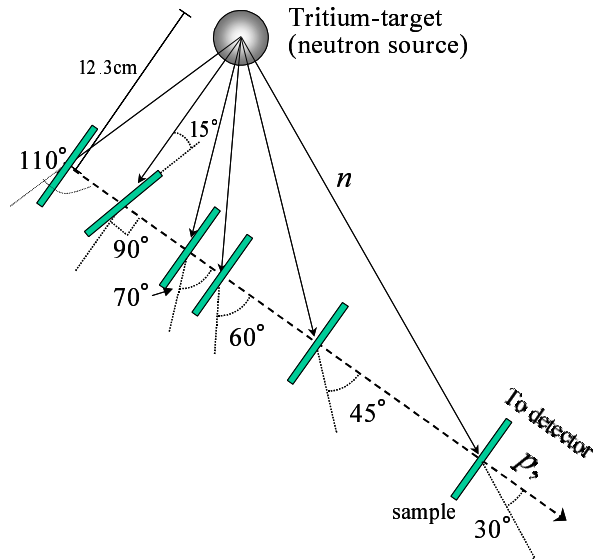


**Fig.2 The sample position for various emission angle**

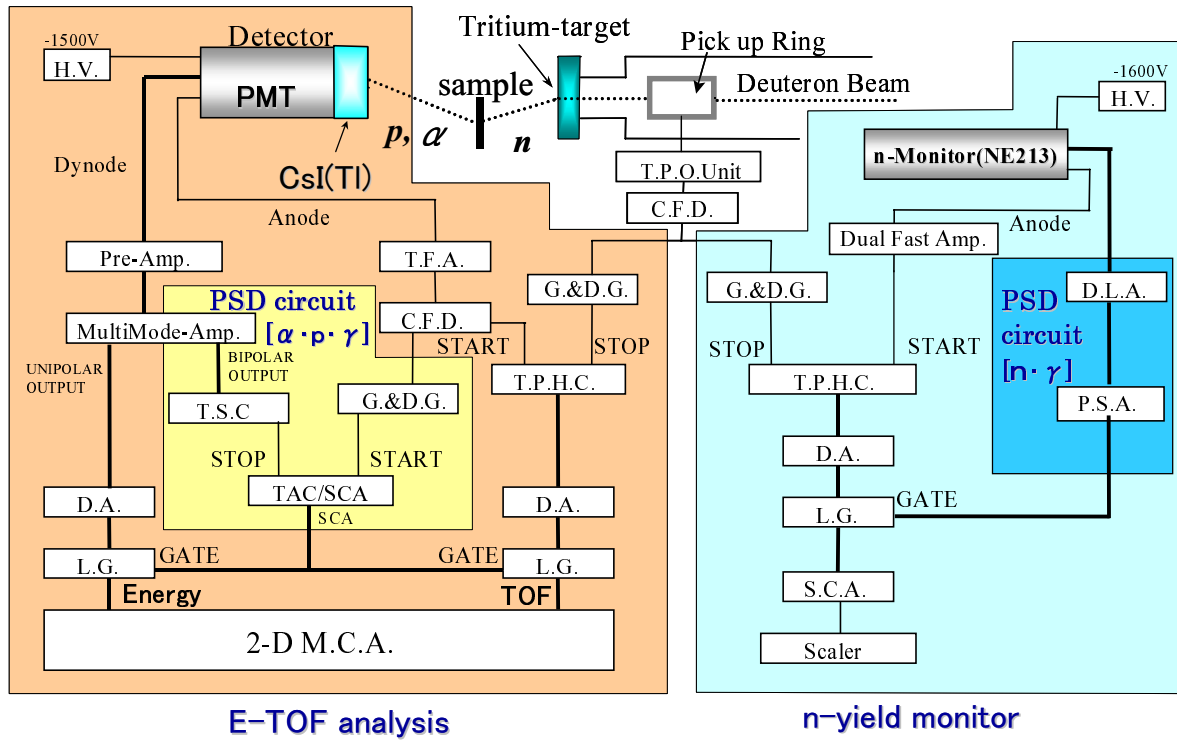


Fig.3 Block diagram of the measuring system

An example of two-dimensional energy and rise time distribution acquired by the CsI(Tl) scintillator is shown in Fig.4. The contours of each particle signals are separated with each other. Thus, we can eliminate the obstructive background and choose a contour of either alpha particles or protons signals by this technique. In addition, since background can be also eliminated with the selected contour zone for either alpha particle or proton in an E-TOF spectrum as shown in Fig.5, satisfactory charged-particle measurement with low background was realized. The principle of two-dimensional E-TOF analysis for charged particles is understood by the following equation,

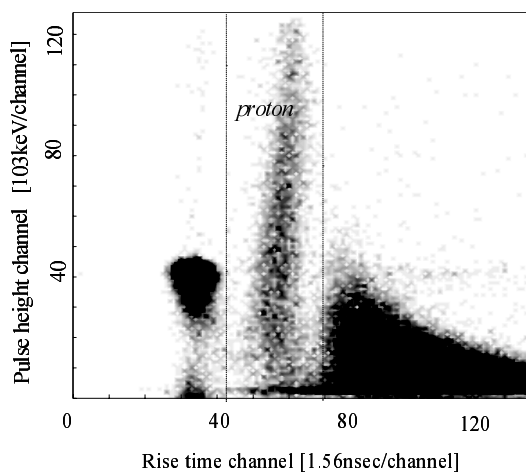


Fig.4 Two-dimensional distribution of rise time and pulse height spectrum

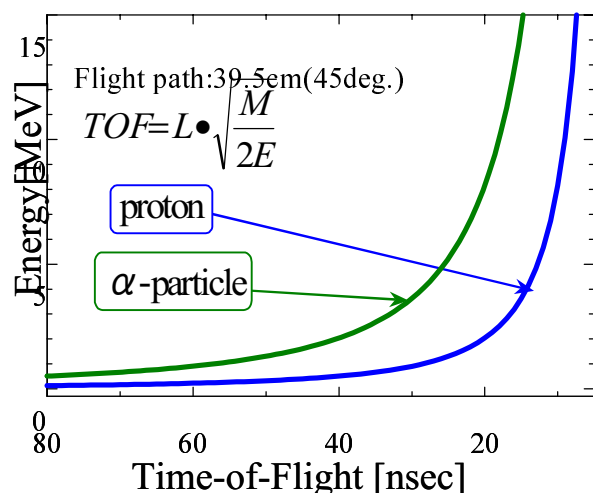


Fig.5 Ideal E-TOF spectra

$$TOF = L \cdot \sqrt{\frac{M}{2E}} \quad (1)$$

where, TOF is the time-of-flight, L the flight path length, E and M the energy and mass of the particle, respectively.

### 3. Data analysis

Figure 6 shows an example of the E-TOF spectrum of proton from  $^{19}\text{F}(n,xp)$  reaction at the emission angle of 45 degree. The spectrum in the background run has been already subtracted from that of the foreground run. Background run was undertaken by removing the sample. Since thick samples were used in this work, background proton produced in the scintillation crystal (CsI) induced by scattered neutrons of source neutrons in the sample was removed. The net energy spectra have been obtained by properly choosing the region of interest around the corresponding ideal curve [Eq.(1)] in the E-TOF spectrum. To deduce DDXs,  $(E_n, E, \theta)$

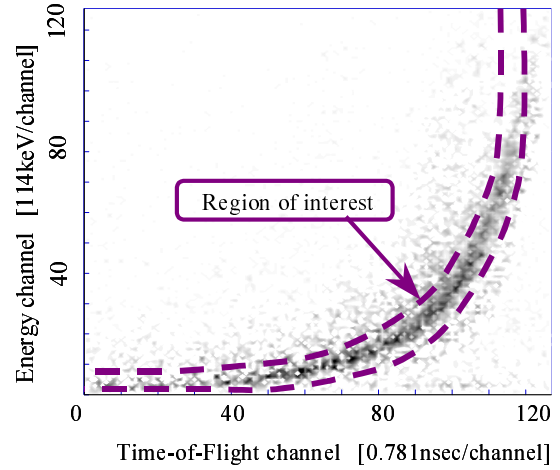


**Fig.6 Measured E-TOF spectrum for  $^{19}\text{F}(n,xp)$  reaction at 45 deg**

[barn/sr/MeV], the net energy spectrum was normalized by comparing the evaluated angular differential cross section (ADX) of  $\text{H}(n,xp)$  with the measured cross section obtained using a polyethylene sample. In proton measurements, the result with the polyethylene sample was also utilized for calibration of the detected proton energy. Finally, the DDX is expressed as the following equation,

$$\sigma(E_n \rightarrow E, \theta) = \frac{r^2 F_p^2}{r'^2 F_p'^2} \times \frac{N'}{N} \times \frac{R(E_n \rightarrow E, \theta)}{\int R'(E_n \rightarrow E, \theta) dE} \times \int \sigma'(E_n \rightarrow E, \theta) dE \quad (2)$$

where, r is the distance between the neutron source and the center of the sample, N the number density of the sample atom,  $R(E_n, E, \theta)$  the net count rate per unit energy of the charged particle emitted from the sample,  $\int R'(E_n, E, \theta) dE$  the total net count of the charged particle for the reference cross section measurement,  $\int \sigma'(E_n, E, \theta) dE$  the reference angular differential cross section of the  $\text{H}(n,p)$  reaction.  $r', F_p'$  and  $N'$  the parameters of the reference polyethylene sample.

The raw DDX data had to be corrected because the broadening functions of angular resolution and the energy loss of the charged particles in the sample were not negligible. In the present work, the spectrum type Bayes estimation method was applied to our charged particle unfolding problem to realize thick sample measurement. This estimation method was recently developed by extending the Bayes theorem [1]. The unfolding procedure is expressed by the following equation,

$$est_j^{(l+1)} = \sum_{i=1}^m \left( d_i \times \frac{est_j^l \times r_{ij}}{\sum_j^n est_j^{(l)} \times r_{ij}} \right), (j=1, n) \quad (3)$$

where,  $r_{ij}$  is the response of detection system which provides the probability of a detection event giving pulse height  $h_i$  for charged particle event  $E_j$ ,  $d_i$  the detected pulse height spectrum,  $est_j^{(l)}$  the estimated spectrum in the  $l$ -th estimation calculation. This formula was repeatedly used for the uncorrected spectrum  $d_i$  in this work. The revised  $est_j^{(l)}$  is used as prior information for the next revise calculation.

#### 4. Results and discussion

The energy differential cross sections (EDXs), angular differential cross sections (ADXs) and total cross sections (TOXs) were deduced by using the measured DDX data. The measured data were compared with the evaluated nuclear data of JENDL fusion file. The experimental results and discussion are described in the following in detail. The comparisons of the total cross sections among the measured data and JENDL-FF are shown in Figs.9 and 12. The TOX value for JENDL-FF used for the comparison was corrected by removing the low energy contribution in the spectra because the charged-particle spectrometer could not measure DDX data for low-energy regions ( $< 3\text{MeV}$ ). In the experimental results, the error bar only includes statistical error.

##### 4.1 Silicon ( $^{nat}\text{Si}$ )

The comparison of the measured DDX data of  $^{nat}\text{Si}(n, xp)$  for the emission angles of 45, 60, 70, 90 and 110 deg and the measured EDX and ADX with JENDL-FF is shown in Figs.7, 8 and 9, respectively. The ADX data were fitted with the legendre polynomials. From

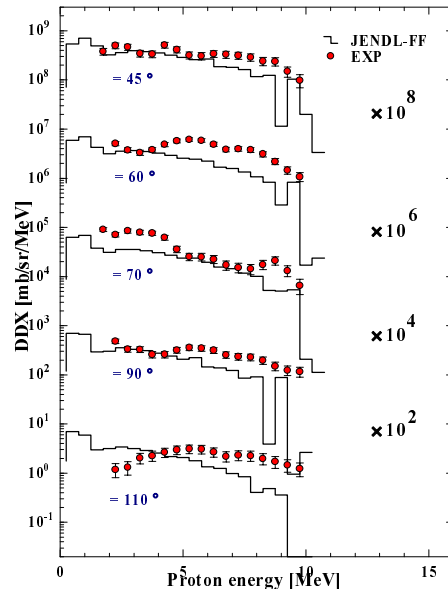


Fig.7 The DDX Data of silicon for the proton emission reaction

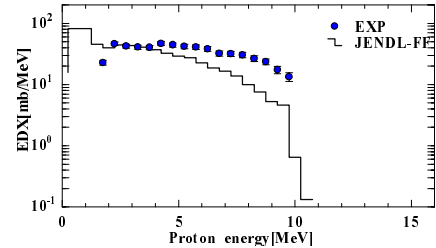


Fig.8 The EDX data of silicon for the proton emission reaction

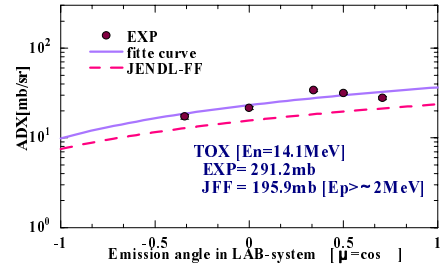


Fig.9 The ADX data of silicon for the proton emission reaction

the comparison of the measured DDX spectra with JENDL-FF, JENDL-FF fairly reproduced the shape of the spectra for forward angles. However, an underestimation was observed in the higher energy region for the EDX spectrum. In the ADX data, JENDL-FF showed a slight underestimation, but the tendency is the same as the experimental result.

## 4.2 Fluorine ( $^{19}\text{F}$ )

The comparison of the measured DDX data of  $^{19}\text{F}(n,xp)$  for the emission angles of 45, 60, 70, 90 and 110 deg and the measured EDX and ADX data with JENDL fusion file are shown in Figs.10, 11 and 12, respectively. From the comparison of the measured DDX and EDX spectra with JENDL fusion file, JENDL fusion file

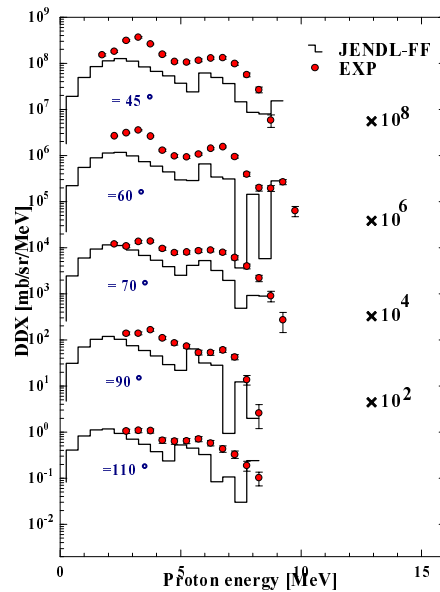


Fig.10 The DDX Data of fluorine for the proton emission reaction

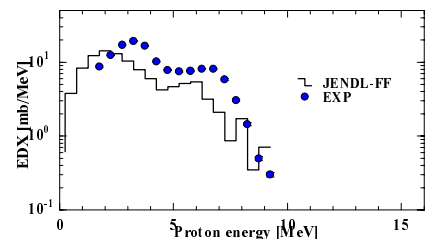


Fig.11 The EDX data of fluorine for the proton emission reaction

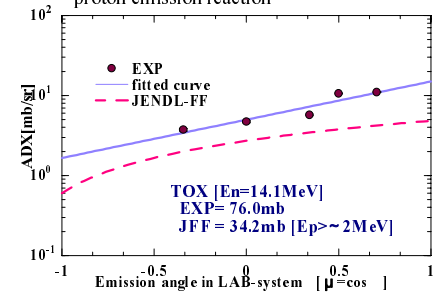


Fig.12 The ADX data of fluorine for the proton emission reaction

fairly reproduced the shape of the spectra, however, an underestimation was observed. In the ADX data, JENDL fusion file showed an underestimation. Also a stronger forward oriented distribution was observed in the experimental ADX compared with the evaluation. In the EDX data, it is presumed that one of the causes of the discrepancy above 3.5MeV is that the  $\text{F}(n,np)$  reaction is underestimated in JENDL fusion file because of deficiency of the experimental data.

## 5. Conclusion

In present study, the measurement of the DDX for proton emission reaction of silicon and fluorine by incident DT neutrons has been carried out at emission angles from 45 to 110 deg. The measured data were compared with evaluated nuclear data of JENDL-FF.

From the comparison of the measured DDX and EDX spectra of  $^{nat}\text{Si}(n,xp)$  reaction with JENDL-FF, An underestimation was observed in the higher energy region especially for the EDX spectrum. In the ADX data, JENDL-FF showed a slight underestimation, but the tendency was the same as the experimental result. For the DDX and EDX spectra of  $^{19}\text{F}(n,xp)$  reaction, JENDL fusion file fairly reproduced the shape of the spectra, however, an underestimation was observed. In the ADX data, JENDL-FF showed an underestimation. Also a stronger forward oriented distribution was observed in the experimental ADX compared with the evaluation.

## Reference

- [1] Iwasaki, S.,: "A New Approach for Unfolding Problems Based Only on the Bayes' Theorem", 9<sup>th</sup> International Symposium on Reactor Dosimetry, Prague, Czech, Sep. 2-6, (1996).
- [2]Takahashi, A., et al.: "A Time-of-Flight Spectrometer with Pulse-Shape Discrimination for Measurement of Double Differential Charged-Particle Emission Cross Section", Nucl. Instr. Meth., A401, 93 (1997).
- [3]Takagi, H., et al.: "Measurement of Double Differential Cross Sections of Charged Particle Emission Reactions by Incident DT Neutrons –Correction for Energy Loss of Charged Particle in Sample Materials–", Proc.1998 Symp. Nul. Data, JAERI-Conf2000-005, 178 (2000).